RSC Advances

Properties and Sodium Salicylate Induced Aggregation Behaviors of Tail-branched Cationic Surfactant With a Hydroxyl-containing Hydrophilic Head

Journal:	*RSC Advances*
Manuscript ID	RA-ART-10-2015-022115.R2
Article Type:	Paper
Date Submitted by the Author:	03-Dec-2015
Complete List of Authors:	Zhang, Yongjie; China Research Institute of Daily Chemical Industry Li, Yunling; China Research Institute of Daily Chemical Industry, Song, Yongbo; China Research Institute of Daily Chemical Industry Li, Jun; China Research Institute of Daily Chemical Industry
Subject area & keyword:	Fine chemicals < Organic

Journal Name

ARTICLE

Properties and Sodium Salicylate Induced Aggregation Behaviors of Tail-branched Cationic Surfactant With a Hydroxyl-containing Hydrophilic Head†

Received 00th January 20xx,
Accepted 00th January 20xx

DOI: 10.1039/x0xx00000x

www.rsc.org/

Yongjie Zhang,[a] Yunling Li,*[a] Yongbo Song[a] and Jun Li[a]

A cationic surfactant with a Guerbet-type branched tail and hydroxyl-decorated head group was synthesized and characterized. Its properties including surface activity, dynamic surface tension, wetting ability, concentration/salt induced aggregation pattern transition and rheological responses of aqueous solution was measured and analyzed. It was found that this new amphiphile possessed powerful surface activity (γcmc = 25.26 mN/m) and could enhance the spreading of aqueous solution on low energy solid surface (paraffin surface); while dynamic surface tension measurement implied that the diffusion rate of surfactant molecules, influenced by the presence of hydroxyl group, had an impact on the wetting process. It was determined that the introduction of branching hydrophobe and hydroxyl into the amphiphilic material crucially contributed to the superior performances. Moreover, the visual transition with increasing concentration of its aqueous solution was observed, while the addition of structure-forming additive sodium salicylate (NaSal) could highly improve the viscosity by inducing the micellar growth in the cationic system which was researched by rheological experiments. Scanning electron microscopy (SEM) and transmission electron microscopy (TEM) were operated to investigate the transformation of aggregates which is responsible for the concentration/salt induced phase behavior transition or rheological responses.

Introduction

It has been an important issue to explore new surfactants with novel structures, because alteration of chemical structures could contribute to unique properties which might have potential applications or theoretical research values.[1] It has well been perceived that nonionic surfactants are more vulnerable to producing low surface energy in aqueous solutions for the absence of electrostatic repulsion between hydrophilic heads. However, very low surface energy could also be achieved by specially modifying the hydrophilic head or changing the hydrophobic structure of ionic amphiphiles.[2-5]

Branched hydrophobic tail could generally enhance the surface activity or other interfacial properties of surfactants.[6-11] There has been a few works that reported extremely low surface energy achieved by introducing branched tail into structure of surfactants. Alexander et al.[5] synthesized a series of anionic surfactants with highly branched single hydrophobic chains and reduced the surface tension to extremely low values (γ_{cmc} = 24 ~ 27mN/m), which is even comparable to certain fluorocarbon surfactants.[12,13] In addition, there are distinct advantages of branched hydrocarbon surfactants over fluorocarbon materials in environmental issues, since fluorocarbons have been suffering limitations from its bioaccumulation and physiological toxicity.[14,15] Moreover, it has been well cognized that the presence of hydroxyl groups on hydrophilic moiety could bring improvement in performance of surfactants,[16-18] since intermolecular hydrogen bonding formed between hydroxyl groups reinforces the interaction between molecules and further influences their aggregation behavior in aqueous solution. Therefore, to incorporate hydroxyl groups into molecules is an important and practical methodology to create new amphiphiles with desirable nature and performances.

In the past two decades, there has been tremendous amount of studies focusing on the viscoelastic micellar solutions generated by cationic surfactant–salt solution systems[19-21] because of their fascinating evolution of nanoscale architectures manipulated by halide anions or other structure-inducing counter ions among which the sodium salicylate is the most extensively used one.[22-24] These facilely tuned self-assembly nanostructures are believed to have potential applications in preparation of microscopic functional materials where microstructured templates are needed.[25,26] A variety of cationic surfactants[27] have been engaged in those studies including cetyltrimethylammonnium bromide (CTAB), cetyltrimethylammonnium chloride (CTAC), cetylpyridinium chloride (CPC) et al. and the morphology of microstructures or the rheological properties are generally modulated by varying

[a] China Research Institute of Daily Chemical Industry, Wenyuan Str. No. 34, Taiyuan, 030001, P.R. China. E-mail: lyunl0068@sina.com; Tel: +86-351-4046827; Fax: +86-351-4040802

† Electronic Supplementary Information (ESI) available: Experimental and spectral data. See DOI: 10.1039/x0xx00000x

the surfactant concentration, salt/surfactant molar ratio and temperature.

In recent years, various cationic surfactants with hydroxyl-contained head groups have been researched, yet the Guerbet-type branched one decorated by hydroxyethyl has never been reported. In this paper, a high performance cationic surfactant Guerbet-cetyl dimethyl hydroxyethyl ammonium chloride (G-CDHAC) was subtly constructed. Compared with our previous work,[28] where a Guerbet branching-contained quaternary ammonium salt (G-CTAC) without decoration of hydroxyl was reported, the presence of hydroxyl group on G-CDHAC improved the surface activity of the Guerbet-type amphiphile to an even higher degree. Therefore, this low surface tension material might have promise in substituting some of the expensive and biologically toxic fluorocarbon materials. In addition, other typical features like wetting ability, dynamic surface tension and self-assembled microstructures, which are correlated with the inherent structure of the new amphiphile and the consequent intermolecular interactions, were also discussed. In order to explore the potential research value of the new material, we investigated the surfactant - NaSal mixed systems of G-CDHAC and G-CTAC by electron microscopy and rheological measurements and some encouraging results were found.

Experimental section

Materials and instruments

Chemicals and materials

Dimethylamine with purity higher than 99% was obtained from Taiyuan Fertilizer Plant, China. Ethylene oxide was obtained from Sinopec Yanshan Co., Ltd (Beijing China). Hydrogen was purchased from Taiyuan Iron & Steel Co., Ltd of China. Sodium salicylate, n-octanol, ethanol, petroleum ether (60-90), acetone and diethyl ether were of analytical reagent grade (A.R.) and purchased from Tianjin University Chemical Experiment Plant and Tianjin Kemiou chemical reagent Co., Ltd.

Experimental techniques

FT-IR spectrum was recorded on a Bruker Vertex 70 FT-IR spectrometer (Germany). ^{1}HNMR spectra were detected by a Varian Inova-400 spectrometer (USA).

Equilibrium surface tension was measured by a KRÜSS K12 Processor Tensiometer (ring method, single measurement) at temperature of 25±0.2^{o}C. Every sample solution was equilibrated for 10min before measurement. Contact angle test was carried out on a KRÜSS DSA255 Drop Shape Analyzer at room temperature (25^{o}C), employing parafilm as solid substrate. Dynamic surface tension was tested by a Krüss BP100 bubble-pressure tensiometer (Krüss Company, Germany), whose range of effective surface age varied from 10 to 200,000 ms. Temperature was maintained to be 25±0.1 °C. Transmittance measurement was operated on a UV-vis spectrophotometer (Lambda-35, Perkin-Elmer) with wavelength set to be 650nm. TEM observation was carried out on a JOEL JEM-1011 (Japan) at an accelerating voltage of 100 kV. Samples of TEM were prepared by immersing an ultrathin carbon-coated copper grid into the micellar solutions, which was then freeze-dried. Field emission scanning electron microscopy (FE-SEM) was carried out on a JEOL JSM-6700F. About 5μL sample was dripped on a silica substrate and then freeze-dried for SEM observation. The rheological measurements were carried out on a HAAKE RS75 rheometer with a cone-plate system (Ti, diameter, 35 mm; cone angle, 1°). The samples were measured at 25 ± 0.2°C with the assistance of a cyclic water bath.

Synthesis

The branched hydrophobic tail of G-CDHAC (whose synthetic route was shown in Scheme S1) stems from Guerbet-cetyl alcohol (2-hexyl-1-decanol), which belongs to a sufficiently researched category of alcohols known as Guerbet alcohol.[29-32] The 2-hexyl-1-decanol in our work was synthesized from n-octanol via Guerbet reaction,[33] which was described in supporting information.

In order to acquire final quaternary ammonium surfactant, the tertiary amine Guerbet-cetyl dimethyl amine was synthesized as intermediate compound by reacting 2-hexyl-1-decanol and dimethylamine. The amination reaction, which has been a mature technology known as one-step amination,[34] was catalyzed by Cu-Ni composite catalyst prepared by co-precipitation.[35,36] Detailed synthetic procedure of tertiary amine was stated in supporting information.

The Guerbet-cetyl dimethyl amine was neutralized by equivalent amount of HCl and subsequently reacted with ethylene oxide at 60-70^{o}C for 3h in an autoclave to produce the cationic surfactant G-CDHAC. Another quaternary ammonium compound Guerbet-cetyl trimethyl ammonium chloride (G-CTAC) was also synthesized by reacting Guerbet-cetyl dimethyl amine and chloromethane at similar conditions (60-70^{o}C, 3h) under the catalysis of Na_2CO_3 as was reported in our previous work.[28]

The final products were firstly purified by extraction, for which the mixture of highly deionized water (75% of volume fraction) and ethanol (25% of volume fraction) was engaged as aqueous phase while petroleum ether was used as oil phase, and then recrystallized from acetone/diethyl ether mixed solvent.

The refined quaternary ammonium salt was detected by water/chloroform bi-phase titration (titrated by sodium tetraphenylborate standard solution, indicated by bromophenol blue), the result of which determined that the average content of cationic active substance is higher than 97wt%. The molecular structure of the G-CDHAC is shown in Figure 1, and the corresponding ^{1}HNMR and FT-IR signals were detected as below:

^{1}HNMR (300MHz, D_2O): 3.98 (br s, 2H, VIII), 3.46 (br s, 2H, VII), 3.29 (br s, 2H, VI), 3.09 (s, 6H, V), 1.87 (br s, 1H, IV), 1.41 (br s, 4H, III), 1.26 (br s, 20H, II), 0.84-0.80 (m, 6H, I); Solvent peak appeared at 4.70ppm. The spectrum was shown in Figure S1.

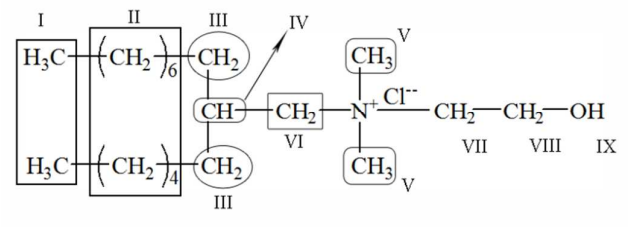

Figure 1. Molecular structure of G-CDHAC and the corresponding signal designation of 1HNMR

Chemical shift of the proton on –OH group was not detected because the active hydrogen exchanges rapidly with D_2O. Thus in order to verify the presence of –OH, ^{1}HNMR was again operated using deuterated DMSO as solvent.

^{1}HNMR (300MHz, DMSO-d6): 5.77 (br s, 1H, IX), 3.84 (br s, 2H, VIII), 3.44 (t, J=4.8Hz, 2H, VII), 3.28/3.29 (d, J=3.6Hz, 2H, VI), 3.10 (s, 6H, V), 1.95 (br s, 1H, IV), 1.32 (br s, 4H, III), 1.26 (br s, 20H, II), 0.88-0.84 (m, 6H, I); Solvent peak appeared at 2.510ppm. as a quintet. The spectrum was shown in Figure S2.

FT-IR: Characteristic peak of O-H stretching vibration appeared at 3369cm^{-1}; Peaks at 2955, 2925 and 2856cm^{-1} are attributed to the symmetric and asymmetric C-H stretching vibrations of CH, CH_2 and CH_3. Bending vibrations of CH_2 and CH_3 were detected at 1465 and 1378cm^{-1}. C-O stretching signal was located at 1048cm^{-1}. The spectrum was shown in Figure S3.

Preparation of G-CTAC/G-CDHAC – NaSal mixed micellar solutions

Stock solutions of 50, 100, and 200mmol/L G-CTAC and G-CDHAC were prepared as well as those of sodium salicylate (NaSal). The concentrations of sodium salicylate solutions were calculated in advance to make the molar ratios of NaSal/G-CTAC (C_S/C_A) and NaSal/G-CDHAC (C_S/C_B) to be 0.2, 0.4, 0.8, 1.0 and 2.0 after mixing. Then stock solutions of surfactants and sodium salicylate were mixed into vials to generate systems with concentrations of 25, 50 and 100mmol/L surfactant, while for each concentration the NaSal/surfactant molar ratios were set to be 0.2, 0.4, 0.8, 1.0 and 2.0. All the samples were equilibrated for at least 2 weeks at 25^{o}C before phase observation and other measurements.

Results and discussion

Equilibrium surface tension

Surface activity is the most basic property of surfactant. The equilibrium surface tension of G-CDHAC aqueous solution as a function of concentration was measured and the result was depicted in Figure 2. It could be interpreted that the G-CDHAC has a powerful ability to decrease the water surface tension to 25.26mN/m (γ_{cmc}). In fact, there should be a limit to which the hydrocarbon surfactants can decrease the water surface tension, and that limit is undoubtedly the air-liquid interfacial tension of the pure liquid hydrocarbon. Considering that the $\gamma_{air\text{-}liquid}$ of n-pentadecane and n-tetradecane are 26.2mN/m and 24.8mN/m respectively,[37,38] the modification on molecular structure in our work has greatly enhanced the potential surface activity of cationic surfactant.

On one hand, the branched structure of hydrophobic tail leaves the water surface to be more densely covered by terminal hydrocarbon groups of surfactant molecules adsorbed on water-air interface, which endows the solution surface with feature like surface of liquid hydrocarbon. On the other hand, intermolecular hydrogen bonding highly enhanced the attracting interaction between interface-adsorbed surfactant molecules due to the presence of hydroxyl group on hydrophilic head, which partially counterbalanced the electrostatic repulsion of positively charged heads (as is illustrated in Scheme 1). Therefore, the interfacial amphiphiles are more tightly packed and consequently minimize the dipolar effect on surface tension because the electrostatic charge on ionic head is greatly shielded.

Other basic parameters of G-CDHAC including critical micelle concentration (CMC), maximum surface excess concentration (Γ_m) and area per molecule at interface (A_0) were analyzed through linear fitting or calculated via equations below

$$\Gamma_m = (-1/2.303nRT) (d\gamma / d\log c)$$

$$A_0 = 1 / \Gamma_m N_A$$

where N_A represents Avogadro's constant, n is set to be 2 considering the subject is a thoroughly dissociated ionic surfactant without addition of other electrolyte. The results are presented in Table 1.

Table 1. Surface adsorption properties of G-CDHAC

parameters	CMC (mmol/L)	Γ_m (10^{-6}mol/m^2)	A_0 (Å^2)
G-CDHAC	2.63	1.84	90.25

It is interesting to notice that the cross sectional area (A_0) of G-CDHAC molecule is smaller than that of G-CTAC (116.5 Å^2 according to reference 28), which is absolutely ascribed to the presence of OH group on G-CDHAC forming hydrogen bonding and further pulling the interfacial amphiphiles to be more closely packed. As a consequence, a higher density of CH_3 groups on water-air interface is correlated with the smaller A_0 value and the contribution of hydroxyl to a lower γ_{cmc} of G-CDHAC than that of G-CTAC is determined.

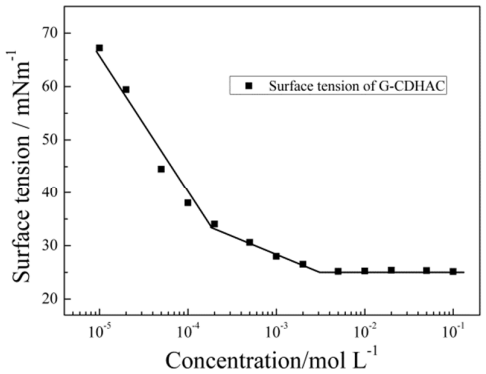

Figure 2. Equilibrium surface tension plot versus concentration.

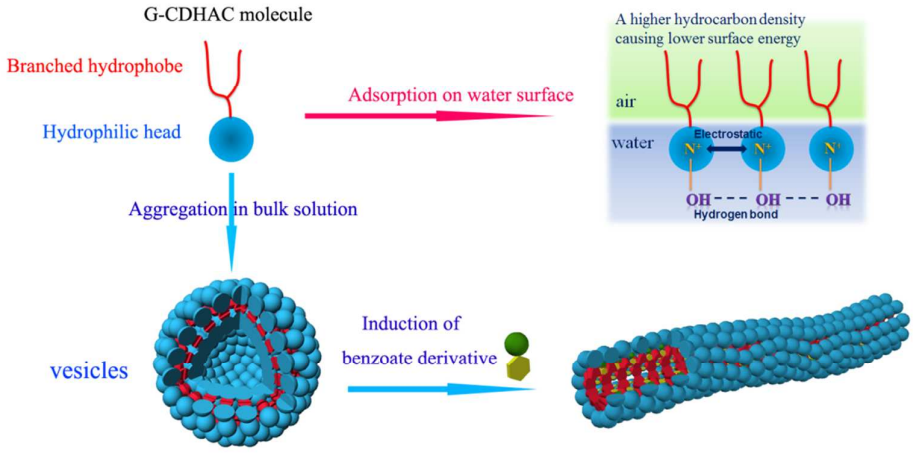

Scheme 1. Illustration of mechanism for low surface energy created by G-CDHAC and for aggregation behaviors in aqueous systems affected by sodium salicylate.

Wetting ability

Wetting ability of G-CDHAC on low energy solid surface was measured by contact angle analysis, the result of which indicated that the new cationic surfactant could enhance the spreading of aqueous solution on paraffin surface (Figure 3). As is shown in Figure 4a, the contact angle could be decreased to lower than 29° at concentration of 100mmol/L. As concentration increased, the wetting ability of G-CDHAC solution was obviously improved and there was a rapid decrease in equilibrium contact angle during concentration range of 0.5~5mmol/L. This phenomenon is in accordance with the description of young's equation:

$$\gamma^{sg} = \gamma^{lg} \cos\theta + \gamma^{sl},$$

where θ is contact angle, and γ^{sg}, γ^{lg} and γ^{sl} represent interfacial energy of solid-gas, liquid-gas and solid-liquid interfaces respectively. While γ^{sg} and γ^{sl} could be presumed as constant due to the internal nature of paraffin and water, cosθ value must increase to equilibrate the equation as the surface tension of solution (γ^{lg}) decreases, which leads to enhanced spreading of liquid drops on solid surface.

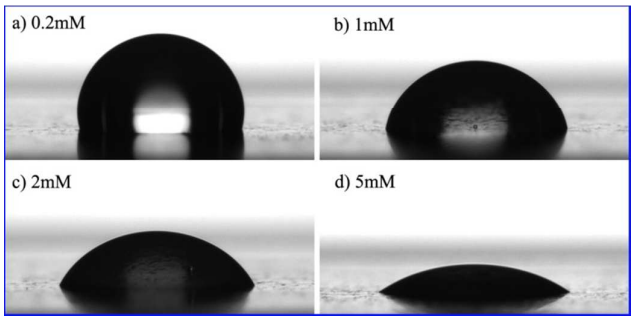

Figure 3. Representative photographs taken by Drop Shape Analyzer which illustrates gradually enhanced spreading of G-CDHAC solution on paraffin surface with increased concentration.

Contact angle curves of solutions at concentrations higher than 5mmol/L exhibited significant decrease in the initial a few seconds, and the decreasing rate was higher for G-CDHAC than it was for G-CTAC,[28] as is depicted in Figure 4b. This is supposed to be correlated with the diffusion of surfactant molecules. Therefore, in order to gain insight into the underlying mechanism of time-dependent wetting process, dynamic surface tension measurement was operated and recorded.

Dynamic surface tension

The dynamic surface tension was detected by bubble pressure method. With time increasing, amphiphiles tend to aggregate onto bubble-solution interface and reduce the bubble pressure, which reflects the decrease of surface tension. It took less time for bubble surface tension to reach equilibrium value at higher concentrations (Figure 5a) because of the accelerated bulk-to-surface diffusion rate. Moreover, it was vindicated to find that the decreasing rate of surface tension for G-CDHAC was higher than it was for G-CTAC in the initial seconds after bubble formation, as could be seen from the curves of dynamic surface tension versus square root of time (Figure 5b). It could be speculated from the result of dynamic surface tension that G-CDHAC molecules diffuse faster to interface, which is consistent with the paraffin-wetting process.

We proposed that the effect of hydrogen bonding between orderly assembled interface-adsorbed amphiphiles and those in subsurface bulky phase reinforced the aggregation potential onto interfacial phase, considering that amphihpiles in bulky solution move in disorder and are in statistically force-balanced state.

Phase behavior observation modulated by concentration/salt addition

Visual appearance change with concentration

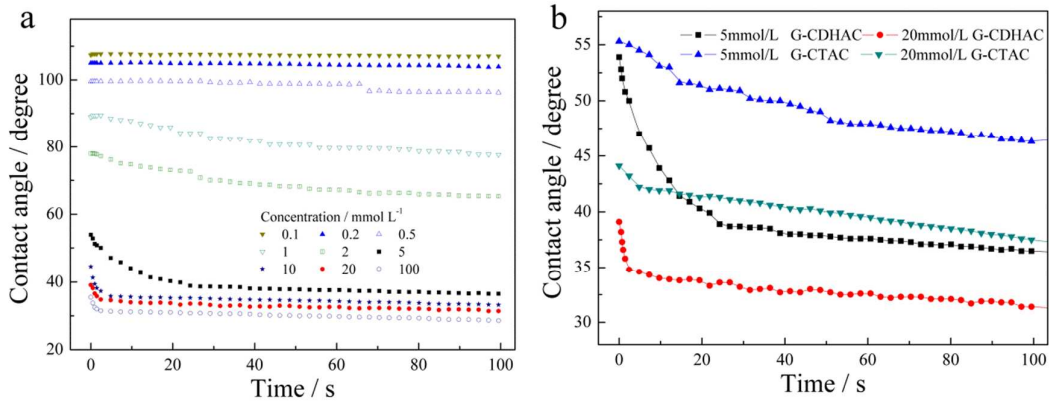

Figure 4. Dynamic contact angle curves as a function of time for (a) different concentrations of G-CDHAC; (b) comparison between G-CDHAC and G-CTAC on their spreading process

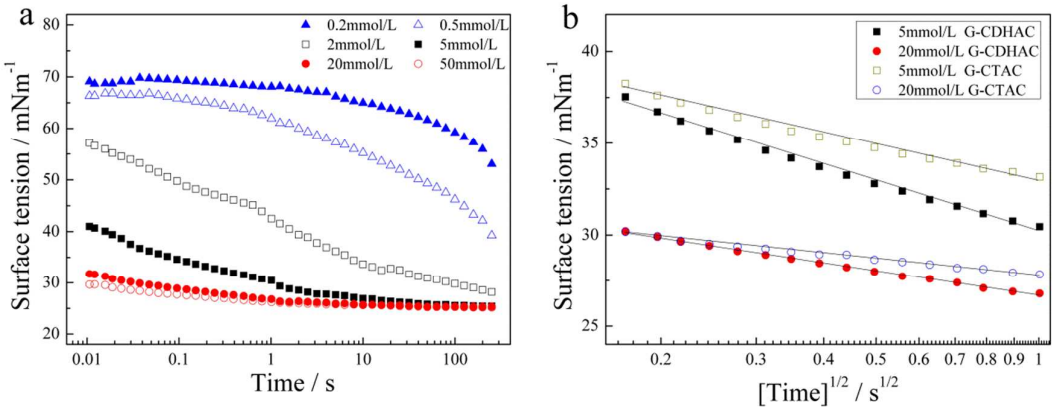

Figure 5. (a) Dynamic surface tension of bubble formed in G-CDHAC solutions of different concentrations and (b) comparison between G-CDHAC and G-CTAC on their decreasing rate of bubble surface tension as function of $[Time]^{1/2}$.

It was interesting to observe that the visual appearance of G-CDHAC solution exhibited transparent-translucent-transparent transition as concentration increased. The aqueous solution became turbid (or blue) during concentration range of 1~10mmol/L without addition of any other substances and Tyndall phenomenon occurred to the turbid solutions irradiated by laser light of 650nm wavelength (Figure 6). Their turbidity was confirmed via transmittance measurement on a UV-vis spectrophotometer (as presented in Figure 6). It could be determined that the sample of 5mmol/L exhibited lowest transmittance and appeared in light blue color. The internal architecture accounting for the turbidity was further investigated by microscopic characterization, as would be discussed below. As the G-CDHAC concentration increased to 20mmol/L or higher, the solution turned transparent again.

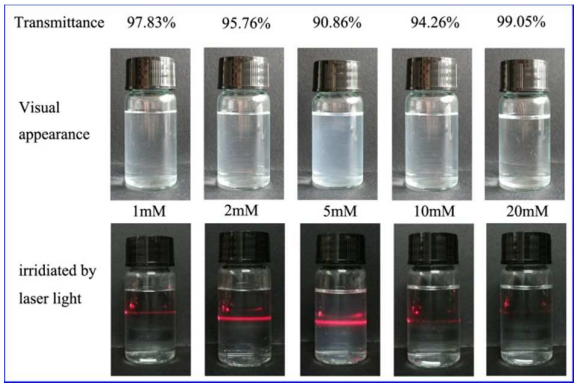

Figure 6. Visual appearance of G-CDHAC solutions changing with concentration and their transmittance for 650nm light detected by UV-vis spectrophotometer.

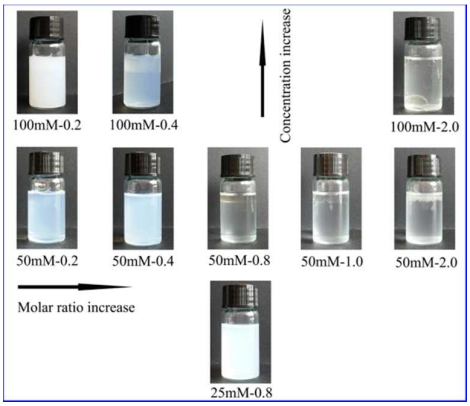

Figure 7. Typical samples of phase behavior transition of NaSal-G-CDHAC mixed systems modulated by concentration and C_S/C_B.

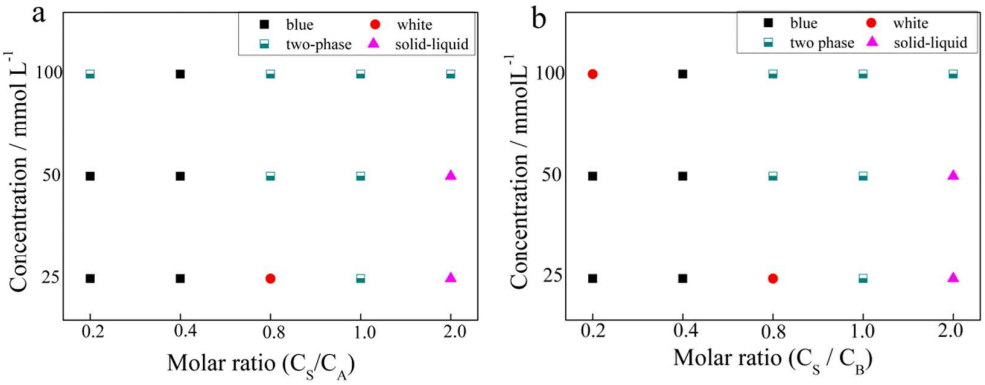

Figure 8. Phase behavior record of mixed systems of (a) G-CTAC/NaSal and (b) G-CDHAC/NaSal.

Phase behavior of G-CDHAC/G-CTAC - NaSal mixed system

Sodium salicylate has been frequently employed to induce the micellar growth of amphiphilic cations (CTA^+, CP^+, etc.), therefore we presume that the newly synthesized cations (G-$CDHA^+$ and G-CTA^+) could also be modulated by this benzoate derivative counter ion to form valuable supramolecular assemblies.

To obtain the concentration and molar ratio where G-CDHAC/G-CTAC-NaSal mixed systems can form homogeneous and stable micellar solutions, macroscopic states of samples were observed and recorded by photography (Figure 7) and phase diagram (Figure 8). It could be seen that the increase of concentration and molar ratio (C_S/C_A for NaSal/G-CTAC, C_S/C_B for NaSal/G-CDHAC) would lead to the creation of two-phase. Moreover, the NaSal-surfactant mixed system was more inclined to be homogeneous while the molar ratio is maintained at 0.4. Figure 7 showed the typical transformation of sample state.

Microscopic investigation

Concentration induced transformation of aggregates

In order to make sense of the visual appearance transition of the G-CDHAC single-component solutions, transmission electron microscope (TEM) was operated on the sample of 5mmol/L G-CDHAC solution which exhibited lowest transmittance. Micrometer-scaled spheres were prevailingly observed in TEM visions (data not shown). Scanning electron microscope (SEM) was also conducted on the freeze-dried sample to confirm the TEM results, and similar spherical assemblies of micrometers were basically detected as expected (Figure 9). Moreover, the SEM images indicated that the micrometer-scale spherical aggregates are composed of nanoparticles incorporated in networks fabricated by nanowires, which is similar with the microstructure found by Chen et al. in their FcM-AOT ionic self-assembled complex.[39] The large size of aggregates explained the translucent appearance of the solution. Besides, the translucent solution stayed unprecipitated for more than 3 months, exhibiting a homogenous solution state, which might be attributed to the effect of Brownian motion and electrostatic repulsion.

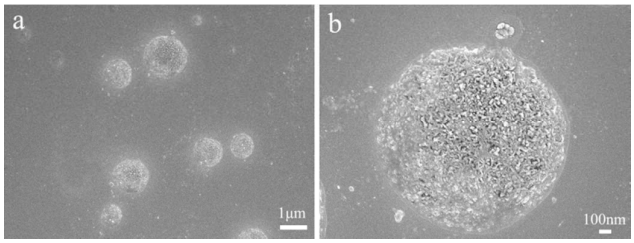

Figure 9. SEM images of micrometer-scaled spherical aggregates formed in 5mmol/L G-CDHAC solution

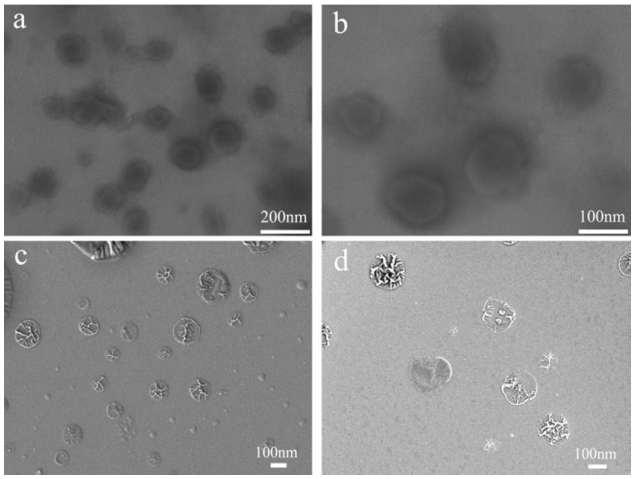

Figure 10. Vesicles formed in 100mmol/L G-CDHAC solution observed by (a, b) TEM and (c, d) SEM techniques.

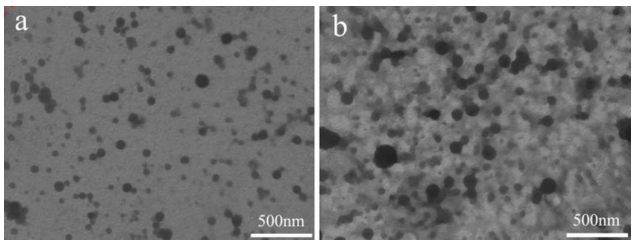

Figure 11. Microscopic characterization of (a) 50 and (b) 100mmol/L G-CTAC/NaSal mixed systems with molar ratio (C_S / C_A) being 0.4.

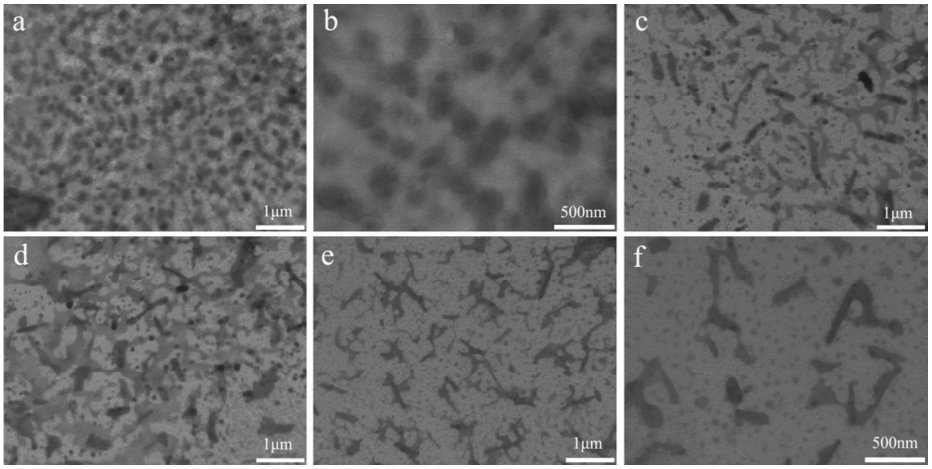

Figure 12. Microscopic characterization of G-CDHAC/NaSal mixed systems with concentrations and molar ratios (C_S/C_B) being (a, b) 25mmol/L and 0.4; (c, d) 50mmol/L and 0.4; (e, f) 25mmol/L and 0.8.

As the G-CDHAC concentration increased to 20mmol/L or higher, the solution turned transparent again and the aggregation pattern of G-CDHAC molecules was confirmed by TEM on concentrated solution of 100mmol/L. As can be seen from TEM visions (Figure 10a, b), the amphiphiles self-assembled into vesicles with diameter of about more than 100nm. The visions observed by SEM confirmed the formation of vesicles (Figure 10c, d), since the wrinkles are clear evidence of collapsed vesicles. It is an extraordinary feature for single-component aqueous solution of mono-alkyl ionic surfactant to self-assemble into vesicles without induction of any other additives, because most of vesicles are formed by double-chained amphiphiles or in systems containing multiple kinds of amphiphiles.[40] Few reports have been issued on spontaneous formation of vesicles by mono-chained surfactant in aqueous solution without addition of negatively charged additives.[41] Therefore, the self-assembly pattern of vesicles is a unique character of the new material.

Microscopic visions of G-CDHAC/G-CTAC-NaSal mixed systems

TEM was employed to characterize the structural transformation of supramolecular assemblies of G-CDHAC and G-CTAC with the tuning of sodium salicylate.

In G-CTAC/NaSal systems, only spherical aggregates could be observed (Figure 11). As the concentration increased from 50 to 100mmol/L, there occurred only increase in the amount of nano-spheres but no further growth or transformation of aggregates. Nevertheless, the shear viscosity of the mixed system was enhanced with the nanoparticles becoming denser at higher concentration, as would be discussed in rheological properties below.

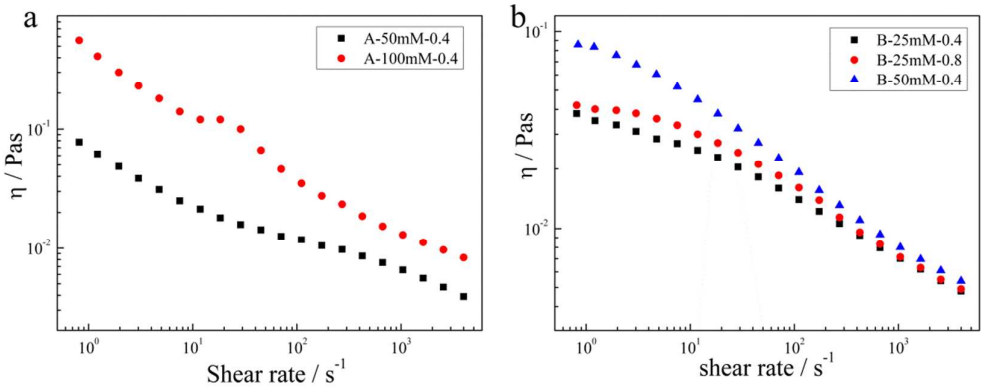

Figure 13. Shear viscosity (η) curves of (a) G-CTAC/NaSal and (b) G-CDHAC/NaSal systems as a function of shear rate.

In G-CDHAC/NaSal systems, there appeared different aggregating behaviors as the concentration or molar ratio varied. In the mixture of 25mmol/L surfactant with molar ratio (C_S/C_B) being 0.4, densely packed nano-particles were observed, some of which aligned in rows and showed a tendency of integrating into nanorods (Figure 12a, b). While the concentration C_B increased to 50mmol/L with a molar ratio of 0.4, wormlike micelles were generated as observed in TEM visions (Figure 12c, d). Further increase of molar ratio to 0.8 could also promote the formation of wormlike micelles (Figure 12e, f). Scheme 1 illustrated the effect of sodium salicylate in inducing the transformation of G-CDHAC aggregates.

Rheological properties

The elongated micellar aggregates might lead to significant rheological responses. For instance, a widely studied viscoelastic system of CTAB/NaSal micellar solutions have been determined to display shear-thinning or shear-thickening properties depending on concentration or salt/surfactant ratios. Therefore we conducted shear viscosity measurements on G-CDHAC/G-CTAC-NaSal mixed systems which showed homogeneous and stable state in phase behavior observation.

It could be seen that the viscosity of the G-CDHAC/NaSal mixed systems was enhanced with the increase of surfactant concentration, while the increasing addition of NaSal (C_S/C_B) could also improve the viscosity (Figure 13b). In addition, all the samples measured exhibited a shear-thinning behavior as the shear rate increased. Cooperation of G-CTAC and NaSal could also enhance the viscosity of aqueous system to different levels depending on the concentration of the mixed system, as is shown in Figure 13a. We speculated that the reinforced aggregation behavior of the cationic surfactants induced by structure-forming agent sodium salicylate, which was discussed in microscopic investigation, should be responsible for the occurrence of rheological responses.

Conclusions

A Guerbet type tail-branched quaternary ammonium surfactant with a hydroxyl-decorated hydrophilic head was synthesized for the first time. This novel cationic amphiphile (G-CDHAC) was found to be an excellent low surface energy material with a γ_{cmc} of 25.26mN/m, while the correlated wetting ability on low energy solid surface was also distinct. The introduction of branching hydrophobe and hydroxylated hydrophilic head was proposed to be responsible for the outstanding performances of the new amphiphilic material. The G-CDHAC molecules formed complex aggregates in dilute solutions with slightly higher concentration than CMC, and formation of vesicles in relatively concentrated solutions without addition of any other inductive agents was confirmed by TEM and SEM techniques. Further investigations concerning salt (NaSal) induced transition of supramolecular assemblies and the consequent response of viscosity properties were also studied, and it was found that the micellar growth in G-CDHAC aqueous system could be achieved by modulating the addition of structure forming agent NaSal.

Acknowledgements

We gratefully acknowledge financial support from the National Science and Technology Support Project of China (No. 2014BAE03B03) and Project for innovation capacity of system-transformed scientific research institute, Ministry of science and technology (2014EG111212)

References

1 B. Song, S. Shang, Z. Song, *J. Colloid Interface Sci.*, 2012, 382(1), 53-60.
2 P. Brown, C. Butts, R. Dyer, J. Eastoe, I. Grillo, F. Guittard, S. Rogers, R. Heenan, *Langmuir*, 2011, 27(8), 4563-4571.
3 A. Mohamed, K. Trickett, S. Y. Chin, S. Cummings, M. Sagisaka, L. Hudson, S. Nave, R. Dyer, S. E. Rogers, R. K. Heenan, J. Eastoe, *Langmuir*, 2010, 26(17), 13861-13866.
4 A. Mohamed, M. Sagisaka, F. Guittard, *Langmuir*, 2011, 27(17), 10562-10569.
5 S. Alexander, G. N. Smith, C. James, S. E. Rogers, F. Guittard, M. Sagisaka, J. Eastoe, *Langmuir,* 2014, 30(12), 3413-3421.
6 Jung, H. T., B. Coldren, J. A. Zasadzinski, D. J. Iampietro, E. W. Kaler, *Proc. Natl. Acad. Sci. USA*, 2001, 98(4), 1353-1357.
7 W. Qiao, Y. Cui, Y Zhu, H. Cai, *Tenside Surfactants Deterg.*, 2012, 49(3), 252-255.
8 C. Huang, Q. Li, M. Li, J. Niu, Y. Song, *Tenside Surfactants Deterg.*, 2014, 51(6), 506-510.
9 R. Varadaraj, J. Bock, P. Valint Jr, S. Zushma, R. Thomas, *J. Phys. Chem.*, 1991, 95(4), 1671-1676.
10 R. Varadaraj, J. Bock, P. Valint Jr, S. Zushma, N. Brons, *J. Phys. Chem.*, 1991, 95(4), 1677-1679.
11 R. Varadaraj, J. Bock, P. Valint Jr, S. Zushma, N. Brons, *J. Phys. Chem.*, 1991, 95(4), 1679-1681.
12 Y. Matsumoto, K. Yoshida, M. Ishida, *Sens. Actuators, A*, 1998, 66(1), 308-314.
13 A. Mohamed, M. Sagisaka, M. Hollamby, S. E. Rogers, R. K. Heenan, R. Dyer, J. Eastoe, *Langmuir*, 2012, 28(15), 6299-6306.
14 T. H. Begley, K. White, P. Honigfort, M. L. Twaroski, R. Neches, R. A. Walker, *Food Addit. Contam.*, 2005, 22(10), 1023-1031.
15 P. Konstantinos, I. T. Cousins, R. C. Buck, S. H. Korzeniowski, *Environ. Sci. Technol.*, 2006, 40(1), 32-44.
16 B. Song, S. Shang, Z. Song, *J. Colloid Interface Sci.*, 2012, 382(1), 53-60.
17 X. Pei, Y. You, J. Zhao, Y. Deng, E. Li, Z. Li, *J. Colloid Interface Sci.*, 2010, 351(2), 457-465.
18 X. Huang, Y. Han, Y. Wang, M. Cao, Y. Wang, *Colloids Surf., A*, 2008, 325(1), 26-32.
19 A. Khatory, F. Lequeux, F. Kern, S. J. Candau, *Langmuir*, 1993, 9(6), 1456-1464.
20 V. K. Aswal, P. S. Goyal, P. Thiyagarajan, *J. Phys. Chem. B*, 1998, 102(14), 2469-2473.
21 B. Šarac, G. Mériguet, B. Ancian, M. Bešter-Rogač, *Langmuir*, 2013, 29(14), 4460-4469.
22 V. Patel, N. Dharaiya, D. Ray, V. K. Aswal, P. Bahadur, *Colloids Surf., A*, 2014, 455, 67-75.
23 M. I. Alkschbirs, A. M. Percebom, W. Loh, H. Westfahl, M. B. Cardoso, E. Sabadini, *Colloids Surf., A*, 2015, 470, 1-7.
24 N. C. Das, H. Cao, H. Kaiser, G. T. Warren, J. R. Gladden, P. E. Sokol, *Langmuir*, 2012, 28(33), 11962-11968.
25 N. S. M. Yusof, M. Ashokkumar, *Soft Matter*, 2013, 9(6), 1997-2002.
26 R. K. Upadhyay, N. Soin, S. Saha, A. Barman, S. S. Roy, *Mater. Chem. Phys.*, 2015, 156, 105-112.
27 W. J. Kim, S. M. Yang, *J. Colloid Interface Sci.*, 2000, 232(2), 225-234.

28 Y. Zhang, Y. Li, Y. Song, J. Li, *Colloid Polym. Sci.*, 2015, DOI: 10.1007/s00396-015-3771-9.
29 A. J. O'Lenick Jr, *J. Surfactants Deterg.*, 2001, 4(3), 311-315.
30 C. Carlini, M. Marchionna, M. Noviello, A. M. R. Galletti, G. Sbrana, F. Basile, A. Vaccari, *J. Mol. Catal. A: Chem.*, 2005, 232(1), 13-20.
31 T. Matsu-Ura, S. Sakaguchi, Y. Obora, Y. Ishii, *J. Org. Chem.*, 2006, 71(21), 8306-8308.
32 J. T. Kozlowski, R. J. Davis, *ACS Catal.*, 2013, 3(7), 1588-1600.
33 China Research Institute of Daily Chemical Industry, *Pat.*, CN103272608A, 2013.
34 H. Kimura, *Catal. Rev.: Sci. Eng.*, 2011, 53(1), 1-90.
35 S. Dong, Y. Li, Q. Li, *Res. Chem. Intermed.*, 2013, 39(3), 869-874.
36 Y. Li, Q. Li, L. Zhi, M. Zhang, *Catal. Lett.*, 2011, 141(11), 1635-1642.
37 W. Shinoda, R. DeVane, M. L. Klein, *Mol. Simul.*, 2007, 33(1-2), 27-36.
38 A. Mejía, M. Cartes, H. Segura, *J. Chem. Thermodyn.*, 2011, 43(9), 1395-1400.
39 Q. Li, X. Chen, X. Wang, *J. Phys. Chem. B*, 2010, 114(32), 10384-10390.
40 X. Guo, H. Li, F. Zhang, S. Zheng, R. Guo, *J. Colloid Interface Sci.*, 2008, 324(1), 185-191.
41 T. Patra, S. Ghosh, J. Dey, *J. Colloid Interface Sci.*, 2014, 436, 138-145.

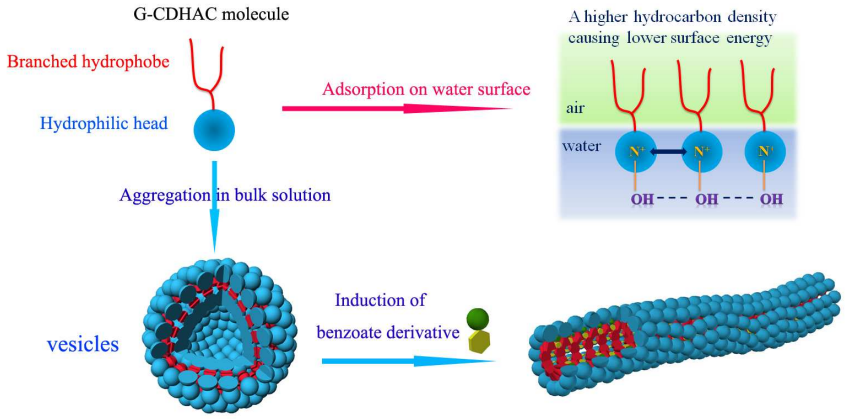

This paper introduced a cationic amphiphile with remarkable surface activity, whose aggregation behavior could be modulated by salt addition.